NASA-CR-203691

a reprint from Applied Optics

Integrating sphere depolarization at 10 μm for a non-Lambertian wall surface: application to lidar calibration

David A. Haner and Robert T. Menzies

The relative Stokes vectors at the detector exit port of a sandblasted and gold-plated integrating sphere are determined for four different polarizations incident on five unique surfaces. The results indicate in all cases that the integrating sphere is a depolarizer. These results validate assumptions used in hard-target calibration methodology for infrared lidars.

Introduction

Lidars in the eye-safe infrared that are used for backscatter and extinction measurements require a method of signal calibration because molecular Rayleigh backscattering is usually below the detection limit. Thus hard-target calibration is used to establish a value for the volume backscattering coefficient.

The volume backscattering coefficient $\beta(\mathrm{m}^{-1}\ \mathrm{sr}^{-1})$ is related to the target reflectance parameter ρ^* for a coaxial lidar configuration by[1]

$$\beta(R_b) = \frac{P_b(t)}{E_{tb}} \frac{E_{ts}}{I_s} \rho^* \frac{O(R_s)}{O(R_b)} \frac{2}{c} \frac{R_b^2}{R_s^2} \cdot \frac{\exp\left[-2\int_0^{R_s} \alpha_s(R')\mathrm{d}R'\right]}{\exp\left[-2\int_0^{R_b} \alpha_b(R')\mathrm{d}R'\right]},$$

where

E_{ts}, E_{tb} is the tranmitted energy for target scattering and backscattering (J),

I_s is the time integral of the target return signal (J),

$P_b(t)$ is the receiver power caused by backscatter (W),

$O(R)$ is the transmitter–receiver overlap function for the particular lidar system,

R_s, R_b is the range of the hard target and to the backscatter volume (m),

α_s, α_b is the total extinction coefficient of the atmosphere appropriate to the scattering process (m^{-1}).

The reflectance parameter for the hard target is further referenced to a standard surface accepted by the research community. Because there are several different techniques of lidar transmitter–receiver construction, there is a need to define the hard-target reflectance parameter with respect to the polarization characteristics of the lidar system. The most common polarizations employed are linear or circular.

To assess the polarized nature of the transmitted radiation, the theory of polarization effects in hard-target calibration utilizes the formalism of Stokes vectors and Mueller matrices.[2] The calibration theory rigorously connects the reflectance of the field target to a standard target through the use of a transfer target. The field target and the transfer target are related through the monostatic reflectometer measurements, whereas the transfer target is related to the standard target by using integrating sphere measurements. The theory makes the assumption that the integrating sphere is a perfect depolarizer in the Stokes–Mueller sense. Further, the general integrating sphere theory usually assumes that the walls of the sphere are Lambertian reflectors,[3–6] i.e., the reflectance is a cosine function of the angle of incidence and the reflected radiance is independent of angle. Evidence of a Lambertian

The authors are with the Jet Propulsion Laboratory, California Institute of Technology, 4800 Oak Grove Drive, Pasadena, California 91109. D. Haner is also a member of the Department of Chemistry, California State Polytechnic University, Pomona, California 91768.

Received 16 September 1992.
0003-6935/93/336804-04$06.00/0.

reflector would be demonstrated if the photometric reflectance function versus the angle from incidence radiation were a cosine function.

The Lambertian assumption for the integrating sphere results in the fraction of the total reflected flux that is incident to be uniform at all points within the integrating sphere.[4] For wall materials that are not Lambertian reflectors, the reflected flux ratio would be some function of the initial incident angle, which could lead to a nonuniformity of the radiance within the sphere.

In our previous experiments on target calibration materials, we found that the material used in the integrating sphere walls (sandblasted aluminum that was gold plated, by Labsphere, Inc., North Sutton, N.H.) was not a Lambertian surface, nor did it have a large depolarization ratio.[7] An experiment was designed to test the assumption that the integrating sphere is an ideal depolarizer. The Stokes vectors describing the incident radiation and the radiation present at the detector were determined for a number of surfaces that had different reflectance characteristics.

Theory

Kavaya[2] showed that the hemispherical reflectance as measured by an integrating sphere $\rho(L3, \mathrm{IS}, \mu_i U)$ can be represented as a linear combination of the Mueller matrix elements (f_{ij}) describing the target material and the Stokes components (I, M, C, S) of the incident radiation, $f_{11}I + f_{12}M + f_{13}C + f_{14}S$. In a similar manner, he showed that the monostatic reflectometer target reflectance parameter, $\rho^*(L3, \mathrm{MR}, \mu_i U_j)$, is another linear combination of the Mueller matrix elements of the target material, the components of the incident radiation, and the polarization properties of the detector. $L3$ is Lambertian type 3 surface, i.e., all 16 Mueller matrix elements are independent of the incident azimuth angle and the reflected polar and azimuth angles. The factors $\mu_i U_j$ relate the combinations of incident (μ_i) and detected (U_j) polarizations; U represents the depolarizing detection property of the integrating sphere, i.e., $[U]$ is the Mueller matrix for an ideal depolarizer, with only U_{11} being nonzero. By taking suitable linear combinations of target parameters representing various incident polarizations and detector characteristics, one relates the reflectance parameters to the integrating sphere reflectance through the same Mueller matrix elements of the target material. The resulting expression for horizontal incident and reflected radiation is given by

$$\rho^*(\mathrm{FT}, LB, hH) = \frac{G(\mathrm{FT}, \mathrm{MR}, hH)}{G(\mathrm{TT}, \mathrm{MR}, hH) + G(\mathrm{TT}, \mathrm{MR}, hV)} \cdot \frac{G(\mathrm{TT}, \mathrm{IS}, hU)}{G(\mathrm{ST}, \mathrm{IS}, hU)}, \cdot \rho(\mathrm{ST}, \mathrm{IS}, hU) k_1 k_2 \cos\phi/\pi$$

where

$G(\;)$ is the signal,
FT is the field target,
TT is the transfer target,
ST is the standard target,
hH is the polarization: incident, reflected-horizontal,
IS is the integrating sphere,
MR is the monostatic reflectometer,
ϕ is the angle of incidence, and
k_1k_2 is the optical correction factors.

This development assumes that the integrating sphere is an ideal depolarizer, i.e., the Stokes vector of the output should have only one component, (E, 0, 0, 0) where $E = f_{11}I + f_{12}M + f_{13}C + f_{14}S$ for any target material and any incident polarized beam. To measure the Stokes components of the radiation from the integrating sphere, one usually employs a polarimeter composed of a retardation plate before a linear polarizer.

Figure 1 shows the schematic of the polarimeter and the definition of the rotation angles for the retarder (β) and the polarizer (α). A polarization-insensitive detector can only respond to the intensity of the radiation, i.e., the first Stokes component. The detector response I' for radiation that has Stokes vector components I, M, C, and S, is incident on the retarder, has retardance Δ, has a reference axis at angle β, and passes through the polarizer with reference axis at angle α is given by[8]

$$\begin{aligned} I'(\alpha, \beta, \Delta) = \tfrac{1}{2}\{I &+ M[\cos 2\beta \cos 2(\alpha - \beta) \\ &- \cos\Delta \sin 2\beta \sin 2(\alpha - \beta)] \\ &+ C[\sin 2\beta \cos 2(\alpha - \beta) \\ &+ \cos\Delta \cos 2\beta \sin 2(\alpha - \beta)] \\ &+ S \sin\Delta \sin 2(\alpha - \beta)\}. \end{aligned}$$

Because this relation is linear in the Stokes components, a sequence of measurements at various α and β may be used to find the vector components.

Experiment

The 10.1-μm radiation, 10 $R(44)$ CO_2 laser line was produced by an Ultra Lasertech CO_2 laser operating in the TEM_{00} mode. The beam was chopped and passed through tandem Brewster plate polarizers to

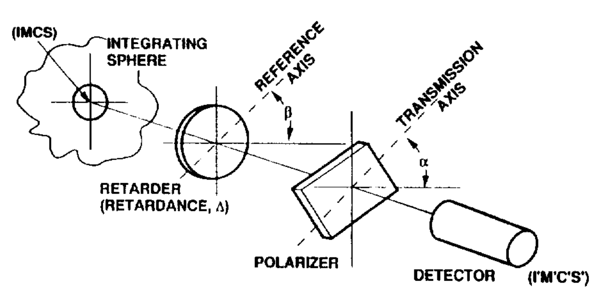

Fig. 1. Polarimeter configuration for measurements of Stokes components of radiation exiting the integrating sphere.

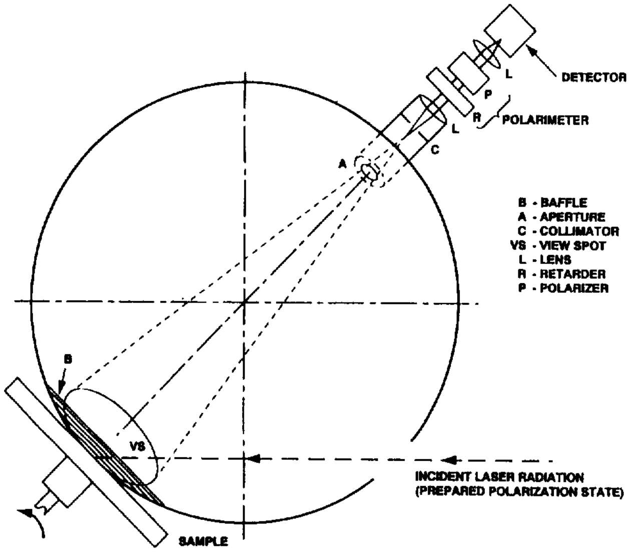

Fig. 2. Layout of the key elements in the integrating sphere and polarimeter–detector optical system.

adjust the beam power, which was monitored by using a calorimetric power meter. The laser beam was usually stable to within 5% over several hours of operation after a warming period. This beam was directed through a quarter-wave plate to change polarization from linear to circular. In each case the beam's Stokes components were measured with the polarimeter to ensure that the incident radiation into the integrating sphere was characterized.

When the beam passed through the integrating sphere, its collimation was checked by noting response while the beam was stopped in a remote Wood's horn, which is known not to produce appreciable reflections. Figure 2 shows the polarimeter detector and collimation optics of the integrating sphere. All the components were rigidly connected to form an assembly. The direct detector field of view inside the integrating sphere is shielded from the first reflection from the target materials by a baffle fixed to the wall.[4] However, the use of two apertures separated by a reflecting cylindrical wall increased the light flux incident on the detector from higher-order reflections within the integrating sphere.[9,10] The pyroelectric detector supplied signals to a phase synchronous detection amplifier, which produced digitized output.

To change the plane of polarization incident on the rotating target materials, we rotated the integrating sphere assembly about the beam line. The target materials selected were Labsphere gold standard, flowers of sulfur with no specular component, flame-sprayed aluminum, sandblasted aluminum, and an antireflection-coated mirror. These targets were rotated at 1 rps and oriented at 45° with respect to the incident beam and relative to the plane of polarization.

To obtain the data used to determine the relative Stokes components of the radiation, we selected nine sets of α, β values for the polarimeter intensity measurements and repeated them four times each. Each set was normalized by the intensity value obtained at $\alpha = \beta = 0$, thus producing relative intensity measurements. This set of eight intensities was divided into two groups of four to obtain values for the Stokes vector components for each group, which were then averaged.

The retardance of the retarder at this wavelength

Table 1. Stokes Components of Integrating Sphere Throughput[a]

Stokes Components	Material: Gold Std.	Material: Flower of Sulfur	Material: Antireflection Mirror	Material: Flame-Sprayed Al	Material: Sandblasted Al	Input Beam Stokes Vector: Ideal	Input Beam Stokes Vector: Real
Perpendicular radiation							
I	1.00	1.00	0.992	1.00	1.00	1	1.01
M	+0.00	−0.00	+0.00	+0.00	+0.00	1	0.992
C	−0.02	+0.01	−0.00	−0.01	−0.00	0	−0.154
S	−0.01	+0.01	+0.00	+0.01	+0.01	0	+0.176
Parallel radiation							
I	1.02	1.00	1.01	1.01	1.01	1	1.01
M	−0.01	+0.0	−0.02	−0.01	−0.01	−1	−0.992
C	−0.02	−0.02	−0.0	−0.0	−0.01	0	−0.154
S	+0.0	+0.0	−0.0	−0.0	−0.0	0	+0.176
Right circular ($\beta = 45$)							
I	1.05	1.04	1.03	1.03	1.03	1	1.11
M	−0.03	−0.02	−0.01	−0.00	+0.01	0	−0.09
C	+0.00	−0.00	−0.00	+0.01	−0.00	0	−0.05
S	+0.02	+0.01	+0.02	+0.01	+0.02	1	1.06
Left circular ($\beta = -45$)							
I	1.04	1.04	1.04	1.03	1.04	1	0.940
M	−0.02	−0.02	−0.01	−0.02	−0.01	0	+0.09
C	−0.01	−0.01	−0.01	+0.00	−0.00	0	−0.09
S	+0.02	+0.02	+0.02	+0.01	+0.02	−1	−0.894

[a]The target angle is 45°.

Table 2. Normalized Integrating Sphere Signals for Various Target Materials at 45° Target Angle[a]

Polarization	Material: Flowers of Sulfur	Antireflection Mirror	Flame-Sprayed Al	Sandblasted Al	Sandpaper (Norton 400)
Perpendicular radiation	0.729	0.960	0.734	0.698	0.090
Parallel radiation	0.737	0.905	0.705	0.652	0.044
Right circular	0.736	0.929	0.713	0.682	0.060
Left circular	0.740	0.935	0.755	0.675	0.064
Linear 45+	0.730	0.938	0.732	0.663	0.071
Linear 45−	0.729	0.947	0.727	0.672	0.072
Average	0.734	0.936	0.728	0.674	0.067
σ_{n-1}	0.005	0.019	0.018	0.016	0.015

[a]The normalized integrating sphere signal is the ratio of the target material signal to the gold standard signal, denoted by S(IS, 10.1 μm, MAT)/S(IS, 10.1 μm, GOLD STD.).

was calculated to be 89.5° by using design parameters provided by the supplier (II–IV Inc., Saxonburg, Pa.). As a further measurement, the polarimeter was removed from the integrating sphere, and values of the reflectance signal ratio for the materials relative to the Labsphere gold standard were obtained for the various incident polarizations.

Results

The results of the polarization measurements for the throughput of the integrating sphere for various input polarizations are presented in Table 1. To analyze the relative error and the polarization characteristics, one should use the intensity properties of the Stokes representation. That is, $I^2 = I_p^2 + I_u^2$, where $I_p^2 = M^2 + C^2 + S^2$ and the subscripts p and u stand for polarized and unpolarized, respectively. The results in Table 1 generally show that the Stokes vector describing the integrating sphere throughput has only one component: the intensity, for all input radiation polarization.

Table 2 shows the integrating sphere signal ratio of the target material to the gold standard, using the detector without the polarimeter for six beam polarizations. These results generally show that the ratio is independent of the polarization of the incident radiation. The values shown for the sandpaper have a greater fractional deviation and are an order of magnitude smaller than the other materials.

Conclusions

The results show that the output of the integrating sphere at the detector has only one Stokes vector component, which proves the depolarization property of the integrating sphere. The depolarization properties of the integrating sphere are complete enough to remove any angular dependence from the highly directional reflectance of the antireflection-coated mirror. These results support the basic assumption used in the formulation of hard-target calibration methodology for infrared lidars developed by Kavaya *et al.*[1]

The result showing the integrating sphere reflectance ratio of the surfaces tested relative to the gold standard to be independent of the polarization of the incident radiation leads to the conclusion that the scattering matrix terms $f_{12} = f_{13} = f_{14} = 0$ for all the surfaces. The depolarization caused by the integrating sphere could be from the angle averaging of the reference direction by the multiple diffuse reflections within the integrating sphere.

The authors acknowledge the technical support of S. Dermenjian and assistance in the data reduction from D. Tratt. The research described here was carried out by the Jet Propulsion Laboratory, California Institute of Technology, under contract with NASA.

References

1. M. J. Kavaya, R. T. Menzies, D. A. Haner, U. P. Oppenheim, and P. H. Flamant, "Target reflectance measurements for calibration of atmospheric backscatter data," Appl. Opt. **22**, 2619–2628 (1983).
2. M. J. Kavaya, "Polarization effects on hard target calibration of lidar systems," Appl. Opt. **26**, 796–804 (1987).
3. D. G. Goebel, "Generalized integrating sphere theory," Appl. Opt. **6**, 125–128 (1967).
4. G. J. Kneissel and J. C. Richmond, "A laser-source integrating sphere reflectometer," Natl. Bur. Stand. Tech. Note **439**, 5–25 (1968).
5. R. Anderson, "Polarized light, the integrating sphere and target calibration," Appl. Opt. **29**, 4235–4240 (1990).
6. M. W. Finkel, "Integrating sphere theory," Opt. Commun. **2**, 25–28 (1970).
7. D. A. Haner and R. T. Menzies, "Reflectance characteristics of reference materials used in hard target calibrations," Appl. Opt. **28**, 857–864 (1989).
8. D. Clarke and J. F. Grainger, *Polarized Light and Optical Measurement*, (Pergamon, Oxford, 1971), Chap. 4, pp. 118–131.
9. W. W. Welford and R. Winston, *The Optics of Nonimaging Concentrators: Light and Solar Energy* (Academic, New York, 1978), Chap. 1, pp. 1–6.
10. K. A. Snail and L. M. Hanssen, "Integrating sphere designs with isotropic throughput," Appl. Opt. **28**, 1793–1799 (1989).